DOI 10.1007/s11015-015-0055-z
Metallurgist, Vol. 59, Nos. 1–2, May, 2015 (Russian Original Nos. 1–2, January–February, 2015)

THREE-DIMENSIONAL MATHEMATICAL (DYNAMIC) MODEL OF THE SINTERING PROCESS. Part II*

Yu. A. Frolov[1] and L. I. Polotskii[2]

UDC 669.162.16

This article presents a three-dimensional mathematical (dynamic) model of the sintering process. The model was developed to solve theoretical and practical problems. It allows real-time determination of the distributions of the temperatures and the chemical compositions of the charge, the melt, the sinter cake, and the gas in the bed of charge materials with allowance for transients. The model also permits real-time determination of the temperatures in the pallets and the parameters of the gas flow (including infiltrating air) in the flue system of the sintering machine.

Keywords: *mathematical three-dimensional (dynamic) model, sintering process, sintering machine, gas, moisture content, reduction, gas dynamics, evaporation, condensation, heating, oxidation, cooling, melting, filtration velocity, temperature, fuel, chemical composition, charge.*

Use of the Mathematical Model for Scientific Purposes. The model that was constructed earlier was used to study heat and mass transfer in the bed of charge materials on a sintering machine at the Chelyabinsk Metallurgical Combine (ChMK). Figure 1 shows the temperature distribution in the bed. The temperature of the material in the upper part of the bed drops sharply immediately after the ignition hearth due to the entry of atmospheric air into the bed and the loss of heat from the bed's surface by radiation.

The air that cools the sinter cake and then enters the combustion zone is heated to 680°C at a depth of 35 mm inside the bed. The maximum temperature of the air (1316°C) is reached 300 mm below the surface of the bed. The charge material reaches its highest temperature – 1343°C – at a depth of 110 mm inside the bed (Fig. 2). The factor that determines heat-transfer efficiency in this part of the bed is the difference in fuel content (3.98% in the upper layer of the bed and 3.14% in its lower part). This underlines the importance of the role played by the segregation of the charge materials based on their coarseness and the corresponding fuel content over the bed's height. Theoretically, it is useful to deliver a high-temperature heat carrier into the bed within the area of the sintering zone that includes the ignition hearth. However, except for supplying the ignition hearth itself with air that has been heated by a low-calorie gas, it is more efficient to recirculate the outgoing gases (a portion of the gases leaving the sintering zone) into the bed to complete the combustion of CO. Recirculating the outgoing gases is preferable because it simultaneously solves heat-engineering and environmental problems.

Figure 3 shows the calculated distributions of the temperatures of the gas and the charge materials over a section of the bed 20 m long. The air is cooler than the material in the upper heat-transfer stage and hotter than the material in the lower stage. The temperature gradient between the gas and the material reaches a maximum of 500°C in the upper stage but is neg-

[1] Uralelektra Scientific and Production Enterprise, Ekaterinburg, Russia; e-mail: uaf.39@mail.ru.
[2] Ural Institute of Metals, Ekaterinburg, Russia; e-mail: mlpol@mail.ru.

* For Part I see *Metallurgist*, No. 12, 1071–1079 (2014).

Translated from Metallurg, No. 1, pp. 27–31, January, 2015. Original article submitted April 21, 2014.

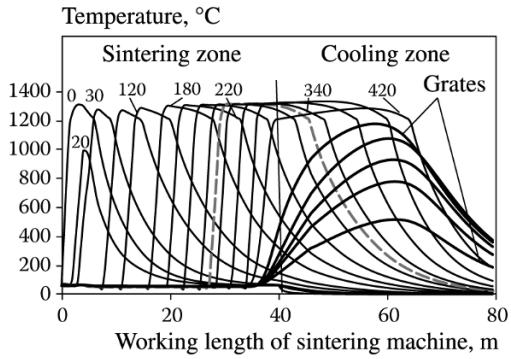

Fig. 1. Temperature distribution over the length and height of the bed and in the grates.

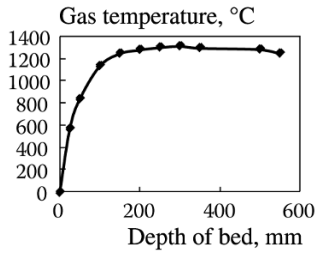

Fig. 2. Change in the temperature of the gas (air) at the inlet of the fuel-combustion zone from the top to the bottom of the bed.

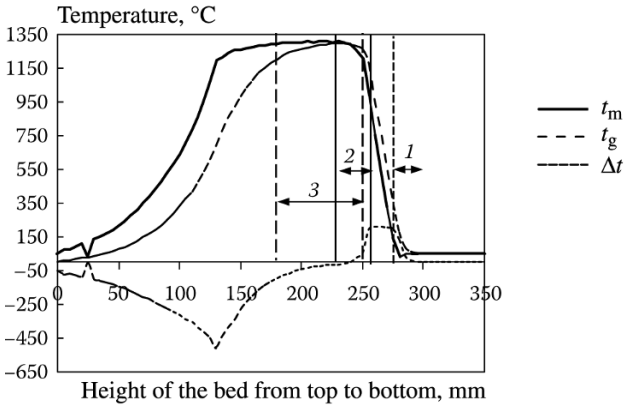

Fig. 3. Distributions of the temperatures of the material and the gas and the temperature gradient between them over the height of the bed: *1*) drying zone, h = 25 mm; *2*) fuel-combustion zone, h = 25 mm; *3*) $CaCO_3$ dissociation region, h = 70 mm; the numbers next to the curves represent the maximum temperature of the gas at the indicated depth of the bed.

ligibly small in the zone where the charge is re-moistened. Heat transfer ceases in the lower stage and – just as importantly – it is completed, since the gas leaves the bed at a lower temperature. The height of the drying zone within the above-indicated section of the bed is 25 mm, while the height of the region in which limestone undergoes dissociation is 70 mm (see Fig. 3).

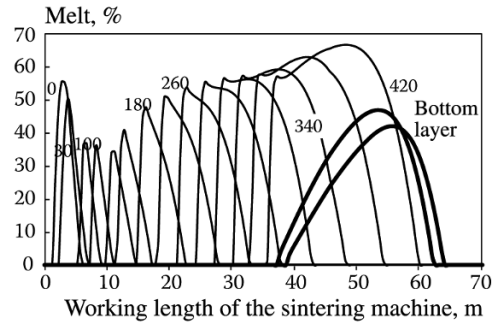

Fig. 4. Distribution of the quantity of molten material over the length and height of the bed.

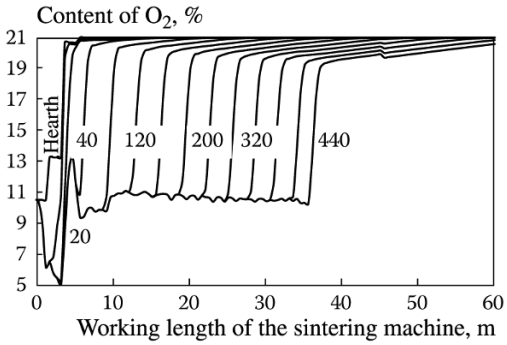

Fig. 5. Distribution of O_2 gas over the length and height of the bed.

At the end of the charge's ignition, the fuel-combustion zone has a height of 35 mm (this value is increased due to a deficit of oxygen). It decreases to 25–30 mm after the charge passes under the hearth. The fuel-combustion zone remains nearly the same over the height of the bed for most of the sintering period. Completion of the drying of the charge at the boundary between the bed and the bottom layer takes place at a distance of 34.25 m along the sintering machine, while combustion of the fuel ends at 38.50 m.

Molten charge materials nearly disappear from the 25-mm-high top zone of the bed 30 sec after the charge's ignition. Atmospheric air enters the zone in the process, but its weight content decreases to as low as 41 wt.% at a depth of 35 mm (Fig. 4). The height of the molten region increases toward the bed's lower boundary in accordance with the temperature distribution, and the melt content of this part of the bed reaches 67%.

As the fuel-combustion zone forms, the O_2 content of the gas leaving the bed (Fig. 5) decreases from 10% under the ignition hearth (under the first section) and from 13% (in the second section) to 5–6% in the hearth gas – at the outlet of the bed. After the bed passes under the hearth, oxygen content increases as a result of the entry of atmospheric air into the bed and subsequently stabilizes at 10.7%. Some of the oxygen (up to 2%) is consumed in the oxidation of FeO in the sinter cake to Fe_2O_3 above the fuel-combustion zone. The deeper the oxygen moves into the combustion zone, the greater the amount of O_2 that is consumed. Thus, the higher the bed, the lower the FeO content of the sinter.

The distribution of CO_2 content in the gas flow over the height of the bed (Fig. 6) rises under the ignition hearth due to dissociation of the limestone. The distribution descends after the hearth and it descends further in the lower part of the bed, which contains less carbon. The height of the $CaCO_3$ dissociation region in the bed changes over its height from 25 mm at the end of ignition to 70–80 mm at a depth of 80 mm inside the bed. The height of this region then stabilizes before the final period of the sintering operation. At the end of the sintering zone, different amounts of unreacted $CaCO_3$ remain in the

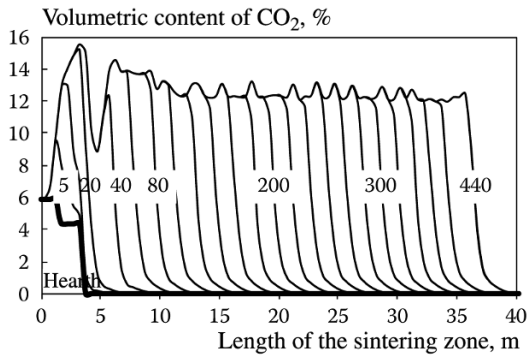

Fig. 6. Distribution of CO_2 gas over the length and height of the bed.

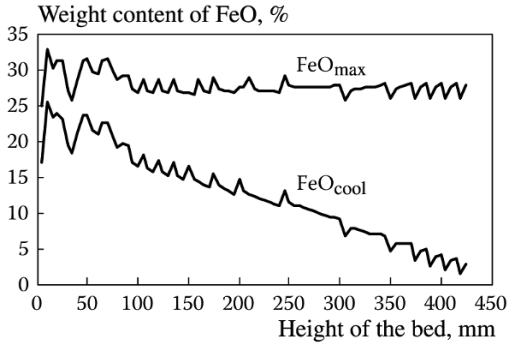

Fig. 7. Distribution of the maximum content of FeO over the height of the bed during sintering and distribution of FeO at the end of the cooling zone of the sintering machine.

55-mm-high portion of the bed next to the bottom layer (the amount of unreacted limestone in this portion ranges from 5% at the top to 67% at the bottom). The dissociation of $CaCO_3$ is completed in the cooling zone 1.7 min after sintering ends.

The maximum FeO content of the combustion zone – where reducing reactions occur – increases from 15.7% in the initial charge to 32% in the top part of the bed. It decreases from the initial value just indicated to 27% in the bed's bottom part. These changes in FeO content are due to the conditions under which ignition and segregation of the charge take place over the height of the bed (Fig. 7). The supply of heat from the oxidation of FeO to Fe_2O_3 under these conditions accounts for 26% of the heat balance of the sintering operation.

Gas filtration velocity (Fig. 8) increases from top to bottom in the bed due to the increase in gas volume that takes place from the evaporation of moisture in the charge and the dissociation of limestone. However, the absolute value of gas filtration velocity decreases during the initial period of the sintering operation due to evaporation of the charge's moisture and an increase in the average temperature of the gas over the height of the bed (to 200°C by the end of ignition). The decrease in the absolute filtration velocity is facilitated by the bed's shrinkage, which is accompanied by a decrease in porosity. After the ignition hearth, gas filtration velocity continuously increases as the height of the zone in which the charge is remoistened (and undergoes an increase in gasdynamic resistance) decreases. As the bed moves into the cooling zone, with a reduced negative pressure, gas filtration velocity at first decreases from 0.415 to 0.340 nm/sec and then increases again. The latter increase is due to a decrease in the average temperature of the sinter cake over its height.

The efficient values chosen for negative pressure in choking the first and second vacuum chambers were 3.5 and 6.0 kPa, respectively. At the beginning of the sintering operation, gas filtration velocity is lower for charges with a higher ini-

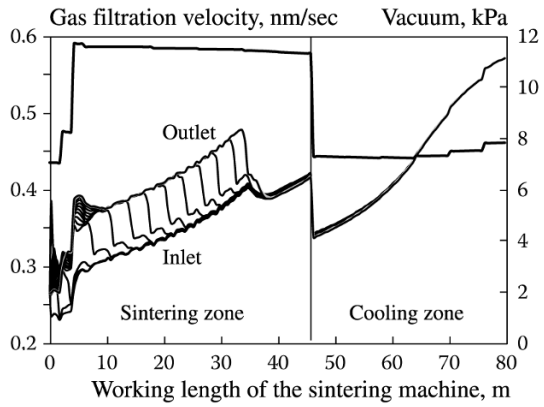

Fig. 8. Change in gas filtration velocity at the inlet and outlet of the bed along the sintering machine.

tial temperature because as condensation takes place in the bed a smaller volume of vapor is transferred to it. In this case, a larger amount of vapor remains in the gas, which increases the volume of the gas and the pressure loss in the bed. The opposite pattern is seen during the main period of the sintering operation, due to drying that the charge has undergone previously. Thus, the higher the initial temperature of the charge, the less the first two vacuum chambers need to be choked.

Many specialists have studied the drying of the charge and moisture condensation during sintering. However, the most detailed studies were conducted by Korotich et al. [1, 2]. The findings from this investigation were used to establish the principles of a theory of these processes. However, the calculations of heat and mass transfer that were performed in this research were based on approximate zonal mass and heat balances. A more rigorous mathematical description of heat and mass transfer was obtained under the guidance of Shklyar [3], although this model did not take fuel combustion and physicochemical changes into account. A theory of drying and moisture condensation that was refined and augmented with the use of a three-dimensional mathematical model was presented in [4].

Below, we relate some of the results that we obtained from the use of a 312-m^2 sintering machine at the West Siberian Metallurgical Combine to illustrate the conditions which exist during sintering.

Our analysis showed that the maximum content of water vapor in the gas decreases from 62 to 37% from the top of the bed its bottom. The vapor content of the gas stabilizes at a depth of 35–40 mm from surface of the bed. The vapor content of the gas and the dew point are redistributed and decrease uniformly over the height of the bed after ignition of the charge. At the beginning of heating, the maximum volumetric vapor content of the dry gas for charges with temperatures of 0, 20, 60, and 82°C is 56, 62, 82, and 118% under the hearth and 22, 27, 37, and 108% at the bottom of the bed, respectively. Conversely, during the main sintering period, the vapor content of the gas decreases as the initial temperature of the charge increases. This decrease can be attributed to the decrease which takes place in the charge's moisture content as a result of its previous drying. For charges with temperatures of 0.20 and 60°C, the rate of advance of the condensation front is 98.117 and 255 mm/min and moisture condensation is completed after 3.76, 3.15, and 1.45 min, respectively.

An increase in the initial temperature of the charge is accompanied by an increase in the maximum value of the dew point. On the other hand, dew point decreases for charges with a higher initial temperature in the main sintering period. Dew point inside the bed undergoes a decrease from 82 to 47°C, this drop including a decrease from 54 to 47°C during the main sintering period.

Moisture condensation is 2.3, 1.73, 0.96, and 0.17% when the initial temperature of the charge is 0, 20, 40, and 60°C, respectively (Fig. 9). Almost no condensation occurs in charges with an initial temperature of 82°C and they begin to dry almost immediately. However, preheating the charge above 60°C is inexpedient due to the sharp deterioration in the conditions for agglomeration of the constituent materials. The 82°C temperature is not theoretical; its value is determined by the temperature and moisture content of the hearth gases. Pre-drying the charge does not fully equalize its moisture content over

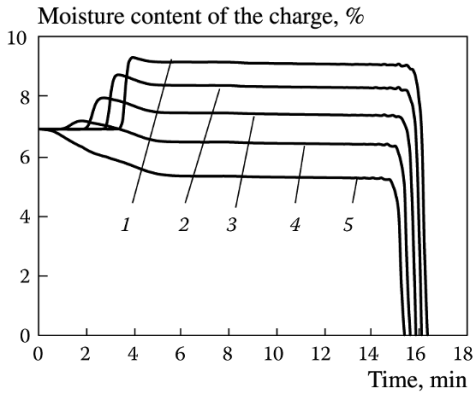

Fig. 9. Change in the moisture content of the charge with different initial temperatures at the lower boundary of the bed: *1*) 0°C; *2*) 20°C; *3*) 40°C; *4*) 60°C; *5*) 82°C.

the height of the bed. Thus, as indicated in [1, 2], there is no stable dew point. Pre-drying the charge causes the relative speed of the drying front to increase as follows with an increase in the initial temperature, rel. %: 0°C – 100; 20°C – 101.4; 60°C – 105.1; 82°C – 114.3.

The initial moisture content of the charge has a significant effect on the extent to which undergoes re-moistening. For example, we obtained the following results, %, for a charge with a temperature of 20°C we obtained the following results:

Initial moisture content	6.50	6.90	7.45
Maximum moisture content over the height of the bed	8.80	9.40	9.85
Maximum moisture content at the bottom of the bed	7.78	8.46	8.87

Thus, the practice of keeping the moisture content of the charge somewhat below the relative value is optimal.

There are three filtration rates during the initial sintering period (Fig. 10): at the inlet of the bed (w_1); at the outlet of the bed (w_2); at the mid-height of the bed (w_3). The first rate characterizes the quantity of hearth gases that can pass through the bed and the corresponding rates of flow of gas and air to ignite the charge. The second rate characterizes the quantity of gas available for the piece of equipment used to choke the vacuum chambers. The third rate – the average rate over the height of the bed together with the bed's drag coefficient and the average temperature of the gas flow over the height of the bed (t_g) – determines the gasdynamic resistance of the bed as a whole.

Use of the Mathematical Model to Solve Practical Problems. Calculations performed with the use of an adapted model [5, 6] established the following: to attain the design capacity (4,500,000 tons of sinter a year) of sinter plant No. 2 at the ChMK from the existing maximum output of 4,011,000 tons (reached during the beginning of the study period) and then increase the plant's capacity to 5,500,000 tons while simultaneously increasing the height of the bed from 430–460 to 550 mm, it is necessary to increase the gas permeability of the bed by roughly 25%, provide the gas-flue system of the sintering machines with a more powerful exhauster (increasing its capacity from 12900 m^3/min to 14500 m^3/min while increasing pressure from 11.0 kPa to 12.5 kPa), and increase the area of the sintering zone by two vacuum chambers at the expense of the machine's cooling zone. To increase the bed's gas permeability, the plant rebuilt the balling drum and the sintering machines' charging equipment. Those changes increased the height of the bed from 460 to 550 mm. The plant also implemented several important measures to modernize its facilities in general [7]. All of these improvements made it possible to increase the unit productivity of the plant from 1.04 to 1.25 tons/(m^2·h) and boost sinter output to 5.2 million tons/yr. Carrying out the recommended reconstruction of the sintering machines will make it possible to completely resolve the existing problems.

For the sinter plant at the Novolipetsk Metallurgical Combine – which has four 312-m^2 sintering machines – it has been recommended that the plant implement an operating system which entails recirculation of 20% of the outgoing gases without diluting them with air. The O_2 content of the recirculating gas will be 16% in this case.

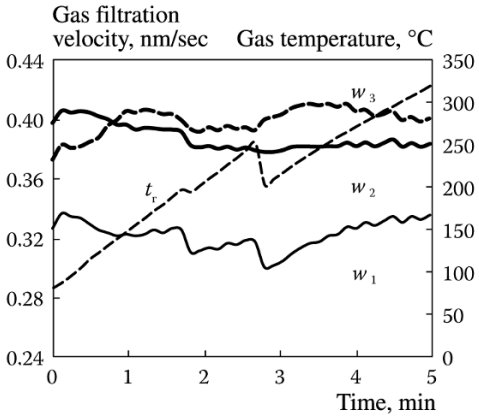

Fig. 10. Change in gas filtration velocity at the inlet (w_1) and outlet (w_2) of the bed and the average value over its height (w_3); average gas temperature over the height of the bed during the initial sintering period with choking of the first two vacuum chambers.

The above mathematical model was used to design a new sintering machine with a total area of 520 m^2. This amount includes 325 m^2 for sintering the charge and 195 m^2 for cooling. Pallet width is 4.4 m and bed height is 700 mm. Two high-pressure (13.5 kPa) 5-MW exhausters with a capacity of 14000 m^3/min are to be installed in parallel for the sintering zone, while two-high-pressure (9.0 kPa) 4-MW exhausters with a capacity of 15500 m^3/min will be provided for the cooling zone.

The model can also be used to create a trainer for training sintering-machine operators.

Conclusion. Thus, the mathematical model that has been developed makes it possible to solve complex practical problems, perform theoretical analyses of the sintering process, and train operating personnel for sinter plants. The model mainly replaces existing local models and balance methods.

REFERENCES

1. V. I. Korotich and V. P. Puzanov, "Formation of the re-moistening zone in suction sintering," *Izv. Vyssh. Uchebn. Zaved. Chern. Metall.*, No. 10, 28–33 (1964).
2. V. I. Korotich, V. P. Puzanov, and Yu. A. Frolov, "Moisture behavior and the gas dynamics of the bed during the initial period of the sintering operation: Reports 1 and 2," *Izv. Vyssh. Uchebn. Zaved. Chern. Metall.*, No 10, 26–30 (1968); No. 12, 37–41 (1968).
3. M. V. Raeva, F. R. Shklyar, and Yu. V. Frolov, "Model of heat and mass transfer during the drying of a porous bed of materials," *Metallurgicheskaya Teplotekhnika: Industry Collection* (1974), No. 2, pp. 154–162.
4. Yu. A. Frolov, V. V. Konoplyanik, G. E. Isaenko, et al., "Analysis of drying, condensation, and the gas dynamics of the bed during the initial period of the sintering operation," *Stal*, No. 6, 5–13 (2008).
5. Yu. A. Frolov, L. I. Polotskii, A. G. Ptichnikov, et al., "Scientific-technical substantiation of the modernization of the sinter plant at the ChMK, with cooling of the sinter on the sintering machines," *Chern. Metall.: Byull. NTiEI*, No. 2, 8–17 (2010).
6. Yu. A. Frolov, A. G. Ptichnikov, V. Kh. Barinov, and N. N. Gorshkov, "Study of the sintering process to modernize sinter plant No. 2 at the ChMK, with cooling of the sinter on the sintering machines," *Chern. Metall.: Byull. NTiEI*, No. 2, 8–17 (2010).
7. A. G. Ptichnikov, V. Kh. Barinov, E. A. Kazantsev, et al., "Improving the efficiency of the sinter plant at the ChMK," *Stal*, No. 7, 6–14 (2011).